대한위생학회지. 제15권 제2호(2000)
Korean J. Sanitation. Vol. 15, No. 2, pp102~111(2000)

The Growth Characteristics of β -$FeSi_2$ as IR-sensor Device for Detecting Pollution Material : The Usage of the Ferrocene-Plasma

Kyung-soo Kim · Il-hyun Jung
Dept. of Chem. Eng., Dankook Univ., San 8, Hannam-dong, Seoul, 140-714, Korea
email : plasmasu@unitel.co.kr

Abstract

As IR-sensor for detecting pollution material, the iron silicide has a fit band gap, high physicochemical stability at high temperature and good acid resistance. The growing film was formed with the Fe-Si bond and the organic compound because plasma resolved the injected precursors into various active species. In the Raman scattering spectrum, the Fe-Si vibration mode showed at 250 cm^{-1}. The FT-IR peak indicated that the various organic compounds were deposited on the films. The iron silicide was epitaxially grown to β-phase by the high energy of plasma. The lattice structure of films had [220]/[202] and [115]. The thickness of the films increased with the flow rate of silane. But rf-power increased with decreasing the thickness. The optical gap energy and the band gap were shown about 3.8 eV and 1.182~1.194 eV. The band gap linearly increased and the formula was below:

$$E_g^{dir} = 8.611 \times 10^{-3} N_o + 1.1775$$

I. Introduction

Recently, infrared-ray sensing technology has taken several objects applicable capability for commercial objects and environmental sensor. In particular, the technology using infrared-ray is applied to remote sensing. A long distance sensing technology is widely applied to the field of science, such as cultivation administration, meteorology, atmosphere physics and environmental problems.

Iron silicide, is widely applied to infrared-ray sensor device for detecting pollution material due to high physicochemical stability at high temperature and good acid resistance[1,2].

Silicides have various phase according to the bonding energy of metal and silicon. Silicide is also classified into metallic and semiconducting silicide. The α and β-phase of iron silicides is thermodynamically steady phase. α-phase is tetragonal metallic silicide ; on the other hand, β-phase formed by phase transformation from α-phase is semiconducting silicide. The band gap(0.87 eV) of β-phase is proper for IR-sensor device[3,4].

Iron silicide has been prepared by Ion Beam

Synthesis (IBS) or Gas Source Molecular Beam Epitaxy (GSMBE). However, the interface of the films are not uniform as a result of an internal diffusion of Fe ions during an annealing process. As the plasma-enhanced chemical vapor deposition (PECVD) induces a reaction in the vapor phase, the fabrication of films using plasma can make better progresses in the quality of the interface of the films[5,6].

In this work, to develop IR-sensor device detecting pollution material, we would know the fundamental physicochemical characteristics of ferrocene-plasma and the formation of the β-phase without annealing process.

II. Experiments

The rf-plasma reactor was used in this experiment(Fig. 1). The surface chemical reaction and the chemical etching generally was occurred by active species in a field of plasma. The interval of substrate and cathode kept 10 cm so that the diffusion rate of active species and the plasma density did not change at the same condition. Pressure before injecting the precursor was maintained at 70 mTorr in the reactor.

Therefore, the deposition reaction did not related with anything except for precursors. During reaction, the reflecting power kept within 5 % for the reproducibility of the experiment.

We used the (111)-oriented, antimony doped n-type, silicon wafer with a resistivity $\rho = 0.1 \sim 100\ \Omega$cm. The organic impurity on the substrate was removed by treating in a solution of $H_2SO_4 : H_2O_2 : H_2O$ (1 : 1 : 2). After rinsing in high purity water, the samples were etched in

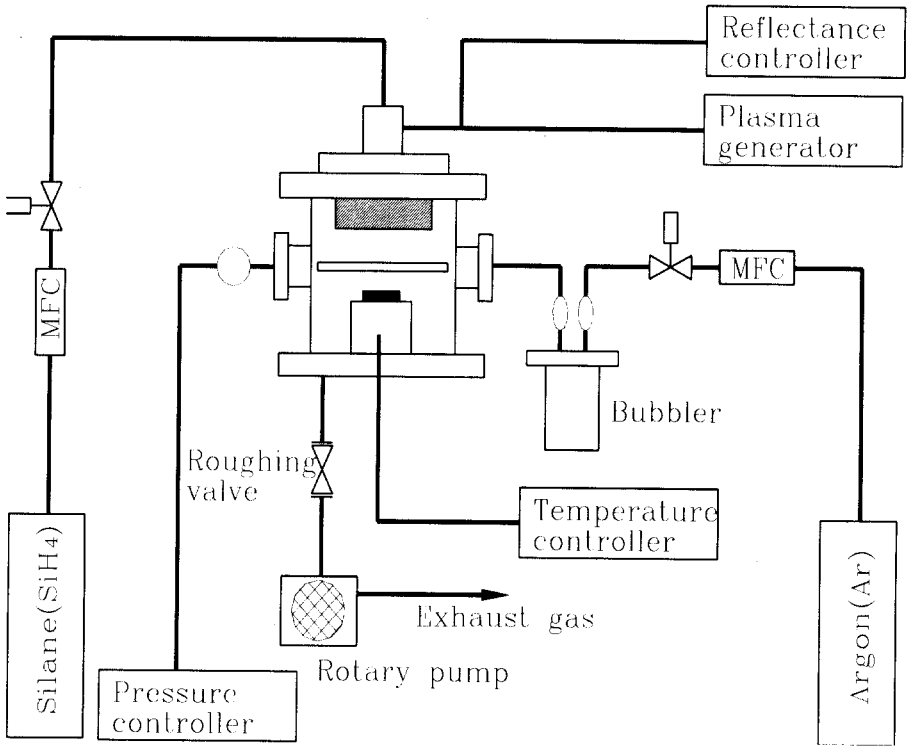

Fig. 1. Schematic diagram of the rf-plasma CVD reactor.

buffered HF : H_2O (1 : 30) for removing the oxide layer (native SiO_2) and then dried by blowing with N_2 gas before loading them into the rf-plasma CVD reactor.

The flow rate of ferrocene was fixed at 10 sccm. After the precursor was injected into reactor, pressure was maintained at 450 mTorr. Ferrocene was injected through a dispersion ring around the substrate by flowing the carrier gas, Ar into the bubbler. The bubbler was heated to 100℃, the vaporizing temperature of the ferrocene.

Table 1. The deposition condition.

Variables	Condition
Reaction time	15~75 min at 280 watt, 300 ℃, 5 sccm SiH_4,
Flow rate of silane	1~5 sccm at 280 watt, 300 ℃, 15 min
Rf-power	160~320 watt at 300 ℃, 5 sccm SiH_4, 15min

Table 1 is the experimental condition. And Table 2 was other analytical instrument used for the characteristics of films prepared by the plasma CVD. The bonding state in the films was observed by FT-IR and the Raman spectra excited with Ar laser. SEM (Scanning Electron Microscopy) was used for observing the thickness and surface of films. The phases determination were detected by XRD (X-ray Diffraction). XRD analysis was carried out using a system for thin solid films and keeping the incident angle of the CuKα source radiation and the range of diffraction angle was from 10° to 90°. The optical properties were calculated from the transmittance measured by UV and near-IR at room temperature.

Table 2. Different analytical instrument used for the characteristics of films.

Properties	Analytical Instruments
Thickness	SEM (Hitachi, S-4100)
Phases determination	XRD (Philips XPERT MPD)
Bonding state	FT-IR (Shimadzu 8501)
Optical properties	Raman (Jasco, NR 1100), UV (HP, USA 8452A) Near-IR (Bio-rad, FTS-60, FTS-40)

Ⅲ. Results and Discussions

The carbon-hydrogen of ferrocene and silane exists as the various active species in plasma. Moreover, the films were grown on a substrate by the active species including carbon-hydrogen and the iron-silicon. The reaction mechanism is

Gas reaction by dissociation and recombination

$$Fe(C_5H_5)_2 + nH_2 \longrightarrow Fe + 2(C_5H_{5+n})$$

$$SiH_4 \longrightarrow Si + 2H_2$$

$$Fe + Si \longrightarrow FeSi$$

$$2(C_5H_{5+n}) + 2H_2 \longrightarrow C_aH_b$$

Deposition reaction of surface

$$FeSi + Si_{substrate} \longrightarrow FeSi_2$$

$$C_5H_{5+n} + Si_{substrate} \longrightarrow SiC_aH_b$$

The ferrocene plasma films deposited on KBr were analyzed with FT-IR to observe the bond structure. Fig. 2 shows the FT-IR results of the bond structure as a function of the reaction time

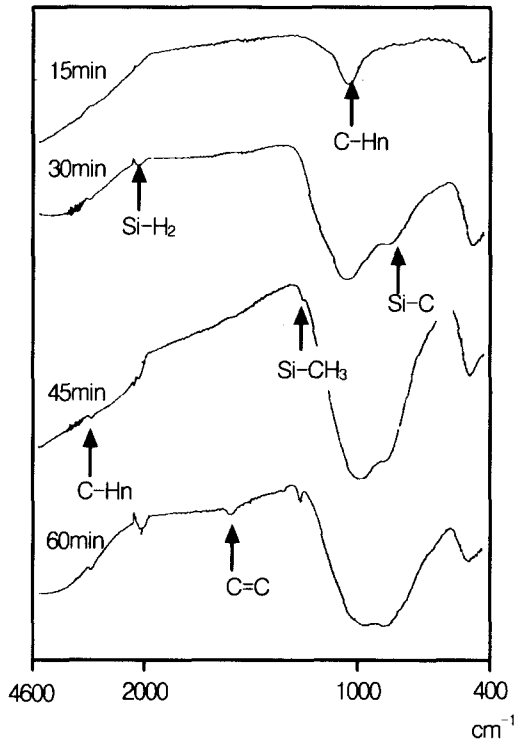

Fig. 2. FT-IR spectrum of Fe-Si films as a function of deposition time at 300 ℃, 280 watt, the ratio of Fe-precursor/silane 2:1 (10 sccm / 5 sccm).

(15 ~75min) at substrate temperature = 300℃, rf-power = 280 watt, and the dilute ratio ferrocene/silane = 2/1 (10 sccm/5 sccm).

At the reaction time 15 min, only $C-H_n$ bond appeared at 1000 cm^{-1}. The peak intensity of C = C, $C-H_n$, Si−C, and $Si-CH_2$ increased with the reaction time.

When the reaction time was 15 min, the XRD pattern was shown in Fig. 3. The β-[202]/[220] and [040] appeared at the diffraction angle 2θ =28°, 47°. If the iron silicide was deposited by ferrocene plasma, β-phase could grow at the low temperature without annealing process.

Fig. 4 shows the FT-IR results of the films as a function of rf-power and the flow rate of silane at the reaction time 15 min. The grown

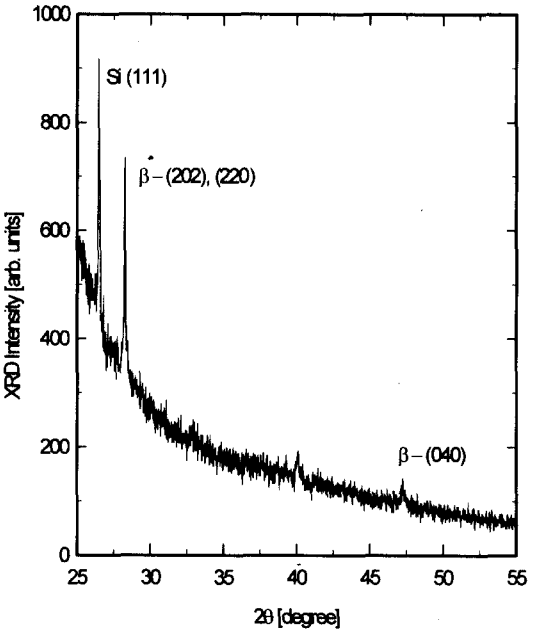

Fig. 3. XRD pattern at the reaction time 15 min.

films included into the organic compounds and the peak appeared at 3100 cm^{-1} $C-H_n$ mode, 1610^{-1} C=C mode, 1400 cm^{-1} C−CH mode and 1100 cm^{-1} $C-CH_n$ mode.

F. Fujimoto, *et al.*[7] and B. J. Jeon,*et al.*[8] introduced that in the process of a-Si:CH and a-Si:H growth, the contents of carbon and hydrogen relatively increased with the flow rate of silane. The deposited films in this work were shown that the contents of carbon and hydrogen increased with the flow rate of silane and rf-power.

The created active species was more dissociated and recombined with increasing rf-power and the flow rate of silane. For this reason, the organic compounds were formed various bonds as such C=C, $C-CH_n$ and the contents of carbon-hydrogen increased with rf-power and the flow rate of silane.

The iron silicide was grown by the surface diffusion of Fe^+ to the dangling bonds created

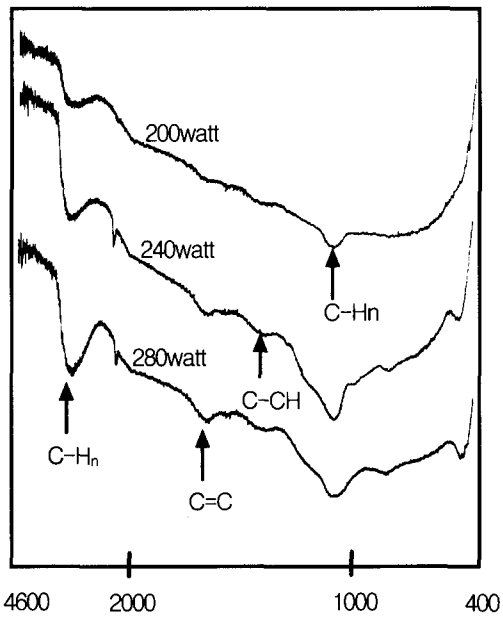

(a)

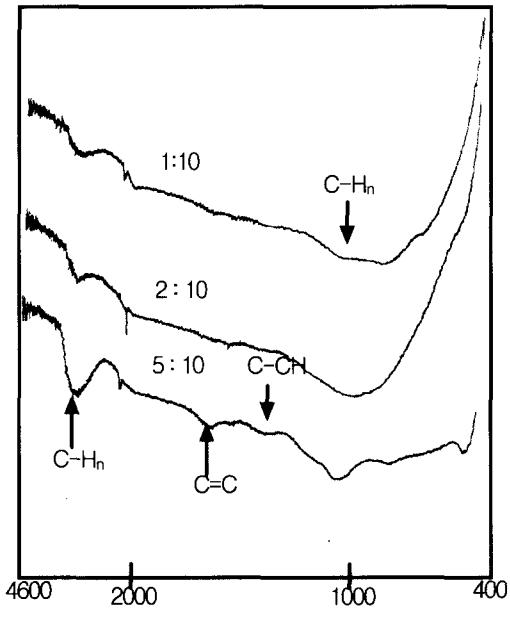

(b)

Fig. 4. FT-IR spectrum of films prepared by rf-plasma CVD as a function of (a) the flow rate of silane and (b) rf-power

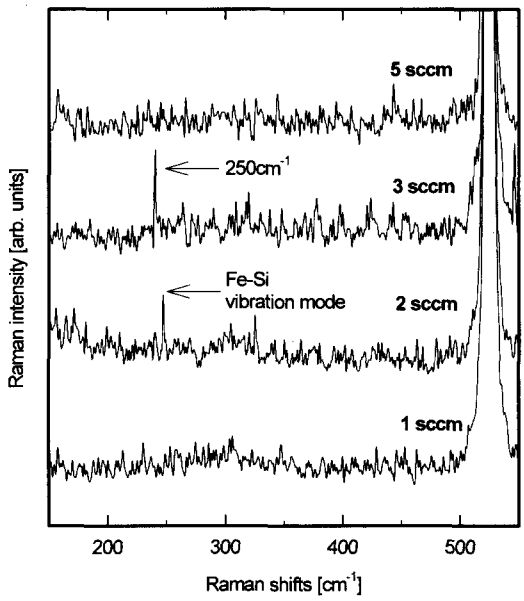

Fig. 5. Raman spectrums of films prepared by rf-plasma CVD as a function of the flow rate of silane at 300 ℃, 280 watt

by desorption of the hydrogen in the films[6].

The lattice defects and the deformation of structure by the diffusion of Fe^{+} induce significant modification of the Raman spectrum, which allows monitoring of the evolution of radiation damage. Moreover, in a different kind of mixed alloy crystal such as SiGe, the frequencies of the Raman phonon mode can determine the degree of alloying, since alloys of silicon and germanium show spectra whose three main line are ascribed to Si-Si, Ge-Ge and Si-Ge atomic pairs[5].

In an alloy of silicon and the iron, such as semiconducting β-$FeSi_2$, the expected vibrational phonon modes are due only to Si-Fe, assuming that the alloy maintains stoichiometric composi- tion. Otherwise, in Si-rich β-$FeSi_2$, another mode due to the Si-Si pair may also appear in the Raman spectra, together with the Si-Fe vibrational mode[5].

Fig. 5. shows Raman scattering spectra ob-

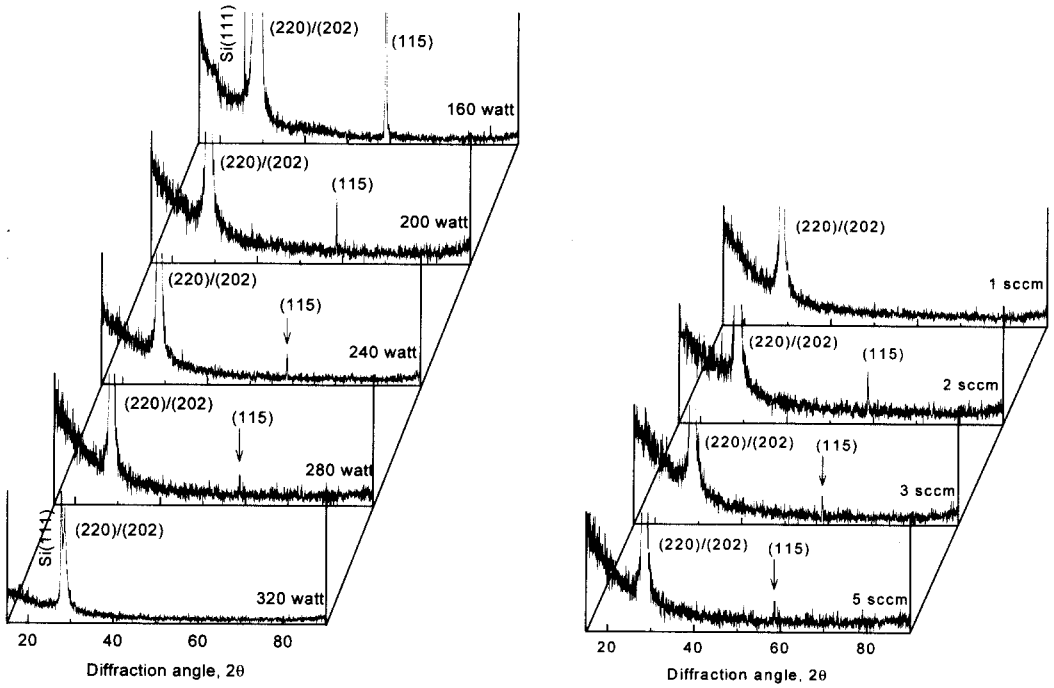

Fig. 6. XRD of films prepared as a function of (a) rf-power and (b) the flow rate of silane by rf-plasma CVD

tained from the films prepared as a function of the flow rate of silane at 300 ℃, 280 watt, 15 min. The vibration mode of Fe-Si appeared at 250 cm^{-1} which reflected the formation of semiconducting β-$FeSi_2$ with good crystallinity. It was predicted from the theoretical calculation on the basis of factor group alanysis, that there are a total of 36 Raman active modes relevant to the Fe-Si pair, which may be differentiated into 12 internal modes (corresponding to atoms moving differently inside the molecule) and 24 external modes (the molecules move as a unit)[5].

The internal modes presumably gave rise to the peak at 250 cm^{-1} observed in this experiment.

One interesting feature in this figure was that a signal at 524 cm^{-1}, which arose from the Si-Si vibrational mode, was observed for all samples. This suggested that this experiment resulted in a deviation of the chemical composition to the Si-rich side, i. e., Si-rich β-$FeSi_2$, presumably through the diffusion of Si atoms underneath the β-$FeSi_2$ layer into the surface.

Fig. 6. shows the XRD pattern of the films grown as a function of rf-power and the flow rate of silane at the reaction time 15 min. For all sample, we could know that the signal from the β-[220]/[202] and β-[115] diffraction was observed at each $2\theta = 29^{\circ}$, 60°. The films could be grown epitaxially on Si [111], where the lattice match with Si varies from depending on the type of Si substrate and its epitaxial relationship to Fe-Si. In the preparation of the films using plasma, the β-phase of silicide

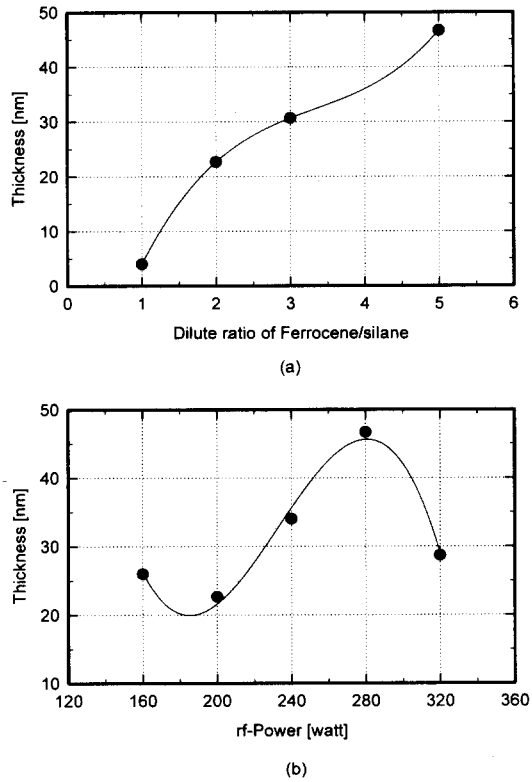

Fig. 7. The effects of (a) the flow rate of silane and (b) rf-power for the deposition rate

could form at low temperature, 300℃ without annealing process.

It was introduced that the phases generally transformed from α to β-phase in the annealing process by the next mechanism of phase transformation[5].

Peritectic reaction (above 865 ℃)
: $\alpha + \varepsilon \rightarrow \beta$
Decomposition reaction (below 860℃)
: $\alpha \rightarrow \beta + Si$
Subsidiary reaction(below 860℃)
: $Si + \varepsilon \rightarrow \beta$

As the reaction mechanism mentioned above, we considered that the α-phase created at low temperature of substrate was decomposed into β-phase and Si. The decomposed Si was

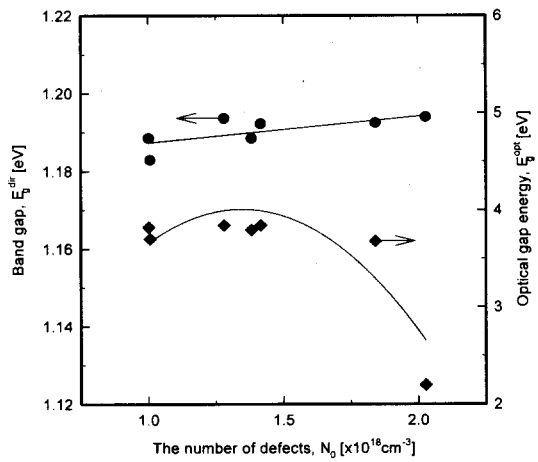

Fig. 8. N_0 vs band gap and optical gap energy

transformed to β-phase by combining with ε-phase between the gas phase of high temperature and the surface of films.

The active species in plasma diffused on the surface of substrate. The surface diffusion rapidly progressed with increasing rf-power but the higher rf-power hindered the surface diffusion as the surface of substrate was etched by the higher rf-power. In Fig. 6, the intensity of β-[115] and [220]/[202] decreased with increasing rf-power as mentioned above.

The thickness of films varied with the condition of plasma and the profile of plasma density. Therefore, the interval of substrate and cathode kept a constant so that the diffusion rate of active species and the plasma density did not change at the same condition.

Fig. 7 shows the thickness of the films prepared at each experimental conditions.

In Fig. 7 (a), since the collision frequency in plasma increased with the flow rate of silane, the concentration of the active species increased. Therefore, the thickness increased from 62 to 700 nm with the flow rate of silane.

In Fig. 7 (b), if the rf-power increased, the large quantity of radical and reactive ion arrived

at substrate since the ionization and the density of plasma increased. But the thickness decreased when rf-power was over 280 watt because the etching reaction was more active than the deposition rate on the substrate.

We obtained the transmittance from the UV spectrum and calculated the optical gap energy of the iron silicide films with applying the method presented by Yoshihiro, *et al*[6]. In addition, as applied in the presented equations, we could calculate the band gap and the number of defects from the transmittance of near-IR spectrum[5]. The optical absorption spectra (α) were determined by measuring their respective transmittance (T) and reflectance (R) spectra and subsequently by computing them using where d is the average thickness of the ferrocene-plasma films.

$$T = (1 - R) \exp(-\alpha d) \quad (1)$$

$$R = (n - 1) / (n + 1) \quad (2)$$

$$\alpha d = \ln(1 - R) / T \quad (3)$$

The optical (equation 4) and direct (equation 5) band gap was calculated by fitting the absorption data to the theoretical curve that follow the relationship between the optical absorption coefficient (α) and photo energy ($h\nu$)

$$\alpha h\nu = B[h\nu - (E_g^{opt})^3] \quad (4)$$

$$\alpha h\nu = A(h\nu - E_g^{dir})^{1/2} \quad (5)$$

The Urbach tail is known that the high concentration of crystalline imperfections or defects in semiconductors creates tail in the distribution of the density of states (equation 6).

$$\alpha_U(h\nu) = \alpha_o \exp\left(\frac{h\nu - E_g^{dir}}{E_o}\right) \quad (6)$$

where α_o is a constant, E_g is comparable to the band gap energy and E_o is an inverse logarithmic slope sof the Urbach tail. The excess absorption $\alpha_{ex}(h\nu)$ due to the sub-band-gap states can be computed from

$$\alpha_{ex}(h\nu) = \alpha(h\nu) - \alpha_o \exp\left(\frac{h\nu - E_g^{dir}}{E_o}\right) \quad (7)$$

where $\alpha(h\nu)$ is the measured absorption data, and the second term

represents the exponential Urbach tails which follow equation (6).

The excess absorption reflects the localized defect densities of states in the forbidden- gap. The number of defects, N_o, can be calculated from

$$N_o = 8.21 \times 10^{16}\left[\frac{1}{f_{oj}} \frac{n}{(n^2 + 2)^2}\right] \times \int \alpha_{ex}(h\nu) d(h\nu) \quad (8)$$

where f_{oj} is the atomic oscillator strength and assumed that f_{oj} is 1.

Table 3. Band gap (E_g^{dir}) and optical gap energy (E_g^{opt}) for films.

Flow rate of silane	E_g^{dir}[eV]	E_g^{opt}[eV]	rf-power	E_g^{dir}[eV]	E_g^{opt}[eV]
1 sccm	1.1890	3.8760	160 watt	1.1885	3.8220
2 sccm	1.1922	3.8420	200 watt	1.1939	2.1980
3 sccm	1.1936	3.8410	240 watt	1.1884	3.7950
5 sccm	1.1829	3.6780	280 watt	1.1829	3.7010
			320 watt	1.1924	3.6780

Table 4. The number of defects No for films.

Flow rate of silane	$N\times10^{18}$ [cm^{-3}]	rf-power [watt]	$N\times10^{18}$ [cm^{-3}]
1 sccm	–	160	1.0015
2 sccm	1.4166	200	2.0278
3 sccm	1.2804	240	1.3820
5 sccm	1.0068	280	1.0068
		320	1.8414

The calculated value was shown in Table 3 and 4. Moreover, in the general process of a-Si:H growth, the content of hydrogen increased with power but the optical gap energy decreased with power[8].

In Table 3, the optical gap energy decreased until rf-power 200 watt. Nevertheless the optical gap energy increased over 200 watt since the concentration of C=C increased with desorbing the hydrogen (see Fig. 4).

The content of carbon-hydrogen increased with rf-power and the flow rate of silane result from the carbon- hydrogen peak in Fig. 4. Moreover, the optical gap energy tended toward decreasing such as showing Table 3. The optical gap was about 3.8 eV and the band gap was shown about 1.182~1.194 eV.

The defect, as such impurities, distortion et al., increased or decreased by the ratio of nucleation. The ratio of nucleation was related with the grain boundary that acted on the barrier of optical properties.

Therefore, since the number of defect acted on the local level in the film, the optical properties had a various value as a function of the number of defect.

In Table 4, the number of defects was very large value and increased with rf-power and the flow rate of silane.

In Fig. 8, the optical gap energy rapidly decreased at a special point since the denser local level was exist by a great number of defect. Probably, the film might possess the new optical properties at the special point. The band gap linearly increased and the formula was below:

$$E_g^{dir} = 8.611 \times 10^{-3} N_o + 1.1775 \qquad (9)$$

The slope showed the band gap for unit defect per unit volume [eV/cm^3] and the y-axis intercept was the ideal band gap of film [eV] that the defect existed in the film.

Ⅳ. Conclusion

In this work, We could confirm that β-phase of silicide was formed at low temperature without annealing process and the lattice oriented to epitaxial growth by high energy of plasma. The quantity of carbon-hydrogen increased with rf-power and the flow rate of silane. If the iron silicide was fabricated by this method, β-phase could grow at the short reaction time and the low temperature without annealing process. The thickness of the films increased from 62 to 700 nm with the flow rate of silane and decreased when rf-power was over 280 watt. The optical gap was about 3.8 eV and the band gap was shown about 1.182~1.194 eV. The number of defects was very large value and increased with rf-power and the flow rate

of silane. The band gap linearly increased and the formula was below :

$$E_g^{dir} = 8.611 \times 10^{-3} N_o + 1.1775 \quad (9)$$

V. References

1. N. E. Christensen, *Physical Review B*, 42(11), 7148(1990)
2. J. Y. Natoli, I. Berbezier, and J. Derrier, *Appl. Phsy. Lett.*, 65(11), 1439(1994)
3. C. A. Dimitriallis, J. H. Werner, S. Logothetidis, M. Stutzmann, and J. Weber, *J. Appl. Phys.*, 68(4), 1726(1990)
4. D. J. Oostra, D. E. W. Nandenhoudt, C. W. T. Bulle-Liennwma, and E. P. Naburgh, *Appl. Phys. Lett.*, 59(14), 1737(1991)
5. H. Katsumata, Y. Makita, N. Kobayashi, H. Shibata, M. Hasegawa, and S. I. Uekusa, *Jpn. J. Appl. Phys.*, 36(5A), 2802(1997)
6. A. Rizzi, B. N. E. Rösen, D. Freundt, Ch. Dieker, and H. Lüth, *Physical Review B*, 51(24), 17780(1995)
7. F. Fujimoto, A. Ootuka, K. Komaki, Y. Iwata, I. Yamane, H. Yamasita, Y. Hashimoto, Y. Tawada, K. Nishimura, H. Okamoto, and Y. Hamakawa, *Jpn. J. Appl. Phys.*, 23, 810(1984)
8. B. J. Jeon, and I. H. Jung *et. al*, *Mater. Chem. and Phys.*, 51, 152(1997)
9. K. Lefki, P. Muret, E. Bustarret, N. Boutarek, R. Madar, J. Chevrier, J. Derrien and M. Brunel, *Solid State Commun.*, 80, 791(1991)